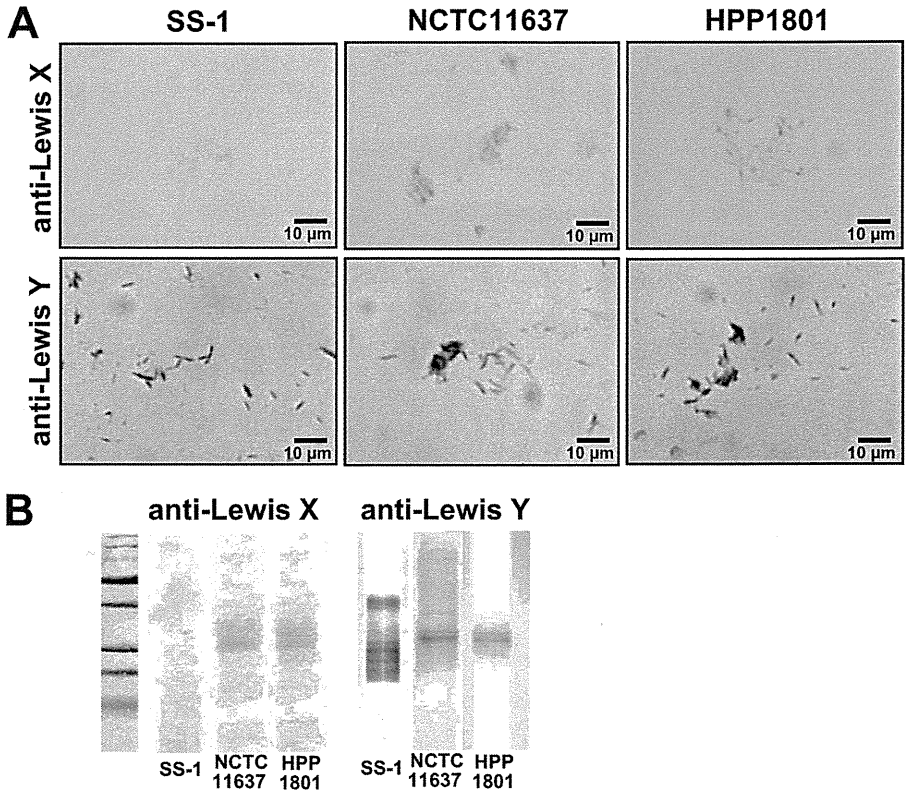

FIG. 9. Detection of *H. pylori* LPS on/in mutant HPP1801 by immunohistological staining and Western blotting. We tried to identify *H. pylori* LPS (Le^x and Le^y antigens) in/on the urease-negative HPP1801 mutant that did not stimulate B-1a cells by anti-Le^x (clone P12) or anti-Le^y (clone F3) murine IgM MAbs. (A) Both Le^x and Le^y were apparently expressed on the surface of mutant HPP1801 as well as isolates NCTC 11637 and SS-1 by light microscopy. (B) Le^x and Le^y antigens were seen in the purified LPS obtained from HPP1801 as well as NCTC 11637 and SS-1 by Western blotting.

the intestinal mucosa detoxifies LPS by dephosphorylating its lipid A with two phosphate groups coupled to glucosamines into a monophosphoryl lipid A that is a 100-fold less toxic than the unmodified version for TLR4 signaling (26). Such a reduction of TLR4 signaling may prevent intestinal inflammation in response to commensal nontoxic microflora. Also, TLR2 on intraepithelial cells enhanced the enzymatic activity of associated protein kinase C by binding to the appropriate ligands in response to luminal bacteria (1); therefore, as we have shown here, innate TLRs may have the ability to distinguish the functional activity of ligands expressed on pathogens. Evolutionary analysis of TLRs and their functional ligands will determine the actual role of TLRs.

Various types of autoantibodies were produced when TLR2 on B-1a cells was stimulated by urease expressed on *H. pylori* without T-cell help. In this case, *H. pylori* urease seems to act as a bacterial endotoxin and TLR2 on B-1a cells recognizes it as a ligand in the production of autoantibodies. Herlands et al. recently suggested a new paradigm of TLR-dependent B-cell initiation of autoimmunity (12). Moreover, two other groups have recently reported similar T-cell-independent activation of autoreactive B cells to produce autoantibodies via B-cell-intrinsic TLR7/9-associated MyD88 signaling, although the actual TLR ligands remain to be elucidated (10, 31). Collectively, as far as we know, our current findings are the first to demonstrate autoantibody production by B cells in a T-cell-independent fashion through the combination of an external TLR with a pathogen-associated ligand.

We have described here that the direct interaction of extracellular TLR2 with *H. pylori* urease as a ligand expressed on the bacterial surface stimulated B-1a cells to produce various autoantibodies in a T-cell-independent manner. This may be why various autoimmune diseases, such as RA (16) and ITP (7), have been associated with *H. pylori* infection. The magnitude of these autoimmune disorders can be manipulated using an anti-TLR2 antibody, such as T2.5, or anti-UB-33-specific antibody if autoantibody production is associated with the interaction between TLR2 and *H. pylori* urease. The findings shown from the current study offer a new notion that *H. pylori* urease is a bacterial endotoxin that can stimulate innate TLR-bearing B-1a cells to secrete a number of autoantibodies and initiate various autoimmune disorders.

ACKNOWLEDGMENTS

This work was supported in part by grants from the Ministry of Education, Science, Sport, and Culture, from the Ministry of Health and Labor and Welfare, Japan, and from the Japanese Health Sciences Foundation and by the Promotion and Mutual Aid Corporation for Private Schools of Japan.

REFERENCES

1. **Cario, E., G. Gerken, and D. K. Podolsky.** 2004. Toll-like receptor 2 enhances ZO-1-associated intestinal epithelial barrier integrity via protein kinase C. Gastroenterology **127**:224–238.

2. **Dempsey, P. W., M. E. Allison, S. Akkaraju, C. C. Goodnow, and D. T. Fearon.** 1996. C3d of complement as a molecular adjuvant: bridging innate and acquired immunity. Science **271**:348–350.
3. **De Vita, S., et al.** 1996. Widespread clonal B-cell disorder in Sjogren's syndrome predisposing to Helicobacter pylori-related gastric lymphoma. Gastroenterology **110**:1969–1974.
4. **Drouet, E. B., et al.** 1991. Characterization of an immunoreactive species-specific 19-kilodalton outer membrane protein from Helicobacter pylori by using a monoclonal antibody. J. Clin. Microbiol. **29**:1620–1624.
5. **Fairweather, D., Z. Kaya, G. R. Shellam, C. M. Lawson, and N. R. Rose.** 2001. From infection to autoimmunity. J. Autoimmun. **16**:175–186.
6. **Feulner, J. A., et al.** 2004. Identification of acyloxyacyl hydrolase, a lipopolysaccharide-detoxifying enzyme, in the murine urinary tract. Infect. Immun. **72**:3171–3178.
7. **Franchini, M., and D. Veneri.** 2006. Helicobacter pylori-associated immune thrombocytopenia. Platelets **17**:71–77.
8. **Futagami, S., H. Takahashi, Y. Norose, and M. Kobayashi.** 1998. Systemic and local immune responses against Helicobacter pylori urease in patients with chronic gastritis: distinct IgA and IgG productive sites. Gut **43**:168–175.
9. **Giannasca, K. T., P. J. Giannasca, and M. R. Neutra.** 1996. Adherence of Salmonella typhimurium to Caco-2 cells: identification of a glycoconjugate receptor. Infect. Immun. **64**:135–145.
10. **Groom, J. R., et al.** 2007. BAFF and MyD88 signals promote a lupuslike disease independent of T cells. J. Exp. Med. **204**:1959–1971.
11. **Hardy, R. R.** 2006. B-1 B cells: development, selection, natural autoantibody and leukemia. Curr. Opin. Immunol. **18**:547–555.
12. **Herlands, R. A., S. R. Christensen, R. A. Sweet, U. Hershberg, and M. J. Shlomchik.** 2008. T cell-independent and Toll-like receptor-dependent antigen-driven activation of autoreactive B cells. Immunity **29**:249–260.
13. **Hildebrandt, E., and D. J. McGee.** 2009. Helicobacter pylori lipopolysaccharide modification, Lewis antigen expression, and gastric colonization are cholesterol-dependent. BMC Microbiol. **9**:258.
14. **Hirota, K., et al.** 2001. Identification of an antigenic epitope in Helicobacter pylori urease that induces neutralizing antibody production. Infect. Immun. **69**:6597–6603.
15. **Iizumi, T., et al.** 2005. Augmentation of Helicobacter pylori urease activity by its specific IgG antibody: implications for bacterial colonization enhancement. Biomed. Res. **26**:35–42.
16. **Ishikawa, N., et al.** 2002. Helicobacter pylori infection in rheumatoid arthritis: effect of drugs on prevalence and correlation with gastroduodenal lesions. Rheumatology (Oxford) **41**:72–77.
17. **Lee, A., et al.** 1997. A standardized mouse model of Helicobacter pylori infection: introducing the Sydney strain. Gastroenterology **112**:1386–1397.
18. **Lu, M., et al.** 2005. Lipopolysaccharide deacylation by an endogenous lipase controls innate antibody responses to Gram-negative bacteria. Nat. Immunol. **6**:989–994.
19. **Meng, G., et al.** 2004. Antagonistic antibody prevents Toll-like receptor 2-driven lethal shock-like syndromes. J. Clin. Invest. **113**:1473–1481.
20. **Monteiro, M. A., et al.** 1998. Simultaneous expression of type 1 and type 2 Lewis blood group antigens by Helicobacter pylori lipopolysaccharides. Molecular mimicry between H. pylori lipopolysaccharides and human gastric epithelial cell surface glycoforms. J. Biol. Chem. **273**:11533–11543.
21. **Moran, A. P., et al.** 2002. Phenotypic variation in molecular mimicry between Helicobacter pylori lipopolysaccharides and human gastric epithelial cell surface glycoforms. Acid-induced phase variation in Lewis (x) and Lewis (y) expression by H. pylori lipopolysaccharides. J. Biol. Chem. **277**:5785–5795.
22. **Nagata, K., et al.** 1992. Monoclonal antibodies against the native urease of Helicobacter pylori: synergistic inhibition of urease activity by monoclonal antibody combinations. Infect. Immun. **60**:4826–4831.

22a. **National Research Council.** 1996. Guide for the care and use of laboratory animals. National Academy Press, Washington, DC.

23. **Paterson, H. M., et al.** 2003. Injury primes the innate immune system for enhanced Toll-like receptor reactivity. J. Immunol. **171**:1473–1483.
24. **Phadnis, S. H., et al.** 1996. Surface localization of Helicobacter pylori urease and a heat shock protein homolog requires bacterial autolysis. Infect. Immun. **64**:905–912.
25. **Rose, N. R.** 2008. Autoimmunity in coxsackievirus infection. Curr. Top. Microbiol. Immunol. **323**:293–314.
26. **Schromm, A. B., et al.** 1998. The charge of endotoxin molecules influences their conformation and IL-6-inducing capacity. J. Immunol. **161**:5464–5471.
27. **Smith, S. M., et al.** 2011. Tribbles 3: a novel regulator of TLR2-mediated signaling in response to Helicobacter pylori lipopolysaccharide. J. Immunol. **186**:2462–2471.
28. **Takahashi, H., K. B. Cease, and J. A. Berzofsky.** 1989. Identification of proteases that process distinct epitopes on the same protein. J. Immunol. **142**:2221–2229.
29. **Takeuchi, O., et al.** 1999. Differential roles of TLR2 and TLR4 in recognition of gram-negative and gram-positive bacterial cell wall components. Immunity **11**:443–451.
30. **Tsai, C. M., and C. E. Frasch.** 1982. A sensitive silver stain for detecting lipopolysaccharides in polyacrylamide gels. Anal. Biochem. **119**:115–119.
31. **Tsao, P. Y., J. Jiao, M. Q. Ji, P. L. Cohen, and R. A. Eisenberg.** 2008. T cell-independent spontaneous loss of tolerance by anti-double-stranded DNA B cells in C57BL/6 mice. J. Immunol. **181**:7770–7777.
32. **Tsuda, M., M. Karita, M. G. Morshed, K. Okita, and T. Nakazawa.** 1994. A urease-negative mutant of Helicobacter pylori constructed by allelic exchange mutagenesis lacks the ability to colonize the nude mouse stomach. Infect. Immun. **62**:3586–3589.
33. **Yamanishi, S., et al.** 2006. Implications for induction of autoimmunity via activation of B-1 cells by Helicobacter pylori urease. Infect. Immun. **74**:248–256.

Editor: A. J. Baümler

APMIS ACTA PATHOLOGICA, MICROBIOLOGICA ET IMMUNOLOGICA SCANDINAVICA

APMIS 120: 56–71

DOI 10.1111/j.1600-0463.2011.02813.x

Characterization of recombinant *Streptococcus mitis*-derived human platelet aggregation factor

HISASHI OHKUNI,[1] HIDEAKI NAGAMUNE,[2] NANA OZAKI,[2] ATSUSHI TABATA,[2] YUKO TODOME,[3] YUKINO WATANABE,[3] HIDEMI TAKAHASHI,[3] KAZUTO OHKURA,[4] HIROKI KOURAI,[2] HIROKI OHTSUKA,[1] VINCENT A. FISCHETTI[5] and JOHN B. ZABRISKIE[6]

[1]Health Science Research Institute East Japan Co. Ltd, Kounosu, Saitama; [2]Department of Biological Science and Technology, Institute of Technology and Science, The University of Tokushima Graduate School, Minami Josanjima, Tokushima; [3]Department of Microbiology and Immunology, Nippon Medical School, Bunkyo-ku, Tokyo; [4]Faculty of Pharmacy, Chiba Institute of Science, Choushi, Chiba, Japan; [5]Laboratory of Bacterial Pathogenesis and Immunology; and [6]Laboratory of Clinical Microbiology and Immunology, Rockefeller University, New York, NY, USA

Ohkuni H, Nagamune H, Ozaki N, Tabata A, Todome Y, Watanabe Y, Takahashi H, Ohkura K, Kourai H, Ohtsuka H, Fischetti VA, Zabriskie JB. Characterization of recombinant *Streptococcus mitis*-derived human platelet aggregation factor. APMIS 2012; 120: 56–71.

We previously purified *Streptococcus mitis*-derived human platelet aggregation factor (Sm-hPAF) from the culture supernatant of *S. mitis* strain Nm-65, isolated from the tooth surface of a patient with Kawasaki disease. Here we produced recombinant Sm-hPAF protein (rSm-hPAF) in *Escherichia coli*, to determine whether rSm-hPAF conserves its platelet aggregation activity. rSm-hPAF precursor (665 amino acids) shows up to 36–56% identity with the family of cholesterol-dependent cytolysins (CDCs), and rSm-hPAF displayed potent hemolytic activity toward mammalian erythrocytes, including human erythrocytes with platelet aggregation activity. The 162-amino acid amino-terminal domain of rSm-hPAF was found in no other CDCs except lectinolysin; this domain is homologous to a portion of pneumococcal fucolectin-related protein. Interestingly, suilysin (SLY) and pneumolysin (PLY) of CDCs also exhibit substantial human platelet aggregation activity, similar to rSm-hPAF, and the platelet aggregation by rSm-hPAF, SLY, and PLY was morphologically confirmed using light and electron microscopy.

Key words: *Streptococcus mitis*; human platelet aggregation factor; suilysin; pneumolysin; Kawasaki disease.

Hisashi Ohkuni, Health Science Research Institute East Japan Co. Ltd, 3-673 Tenjin, Kounosu, Saitama 365-8585, Japan. e-mail: h-okuni@nms.ac.jp

Kawasaki disease (KD), an acute febrile, mucocutaneous, lymph node syndrome, is characterized by systemic vasculitis, including coronary artery aneurysms. The epidemiological features, clinical symptoms, and laboratory findings of KD suggest that an infectious organism resident in the oral cavity or throat acts as the etiological agent, releasing toxic products that can cause inflammatory reactions and immunological disorders (1–6).

To address this hypothesis, we isolated numerous species of bacteria that could produce extracellular immunobiologically active factors from KD patients and age-matched non-KD patients with febrile diseases such as pharyngitis, viral pneumonia, etc. (3, 4, 7). Most of these organisms were identified as viridans streptococci, predominantly *Streptococcus mitis* and

Received 9 March 2011. Accepted 3 August 2011

S. oralis by DNA–DNA hybridization with type-strain DNA and by *sodA* sequence clustering (8). We detected a factor that aggregated human blood platelets in the culture supernatants of some *S. mitis* strains isolated from the oral cavities of patients with and without KD (7), and purified it from the culture supernatant of *S. mitis* strain Nm-65, isolated from a KD patient [strain O-85 in (9)]. The purified factor (*S. mitis*-derived human platelet aggregation factor, Sm-hPAF) had a molecular weight of approximately 66 kDa by sodium dodecylsulfate-polyacrylamide gel electrophoresis (SDS-PAGE) and an isoelectric point of approximately 8.5. Native Sm-hPAF (nSm-hPAF) had an absorption peak at 278 nm, contained no sugars, and began its amino-terminal sequence with *N*-DEQGNRPVETENIAR (9). Sm-hPAF also exhibited hemolytic activity toward human erythrocytes.

Here we compare the partial characterization of recombinant Sm-hPAF (rSm-hPAF) with the analysis of nSm-hPAF to determine the similarities between the hemolytic and platelet aggregation activities of the two proteins. Homology analysis showed that rSm-hPAF is closely related to the cholesterol-dependent cytolysins (CDCs) (10), a family of the pore-forming cytolysins (11), and the amino-terminal 162 amino acids of Sm-hPAF are homologous to a portion of the pneumococcal fucolectin-related protein (GenBank accession number AE007504). Additionally, we found that CDC family members such as pneumolysin (PLY) and suilysin (SLY) also possessed human platelet aggregation activity.

MATERIALS AND METHODS

DNA extraction

Streptococcus mitis strain Nm-65 and *S. suis* strain GTC430 (type strain ATCC437650) were cultured in chemically defined medium at 37 °C for 16 h under 5% CO_2, as previously described (9). Bacterial cells were harvested by centrifugation at 8500 *g* for 15 min and washed with 50 mM EDTA (pH 7.8). The cells were boiled at 100 °C for 5 min and suspended in 10 mM Tris-maleate-NaOH (TMN) buffer (pH 7.0). Then, *N*-acetylmuramidase SG (Seikagaku Corporation, Tokyo, Japan) was added to a final concentration of 100 μg/mL in TMN buffer. The cell suspension was incubated at 50 °C for 1 h followed by addition of SDS (Wako Pure Chemical Co., Osaka, Japan) to a concentration of 1%. After protoplast/spheroplast burst, chromosomal DNA was purified according to the method of O'Connor and Cleary (12).

Mixed oligonucleotide-primed PCR

The nucleotide sequences of PCR primers and probes for the cloning of *sm-hpaf* are given in Table 1. Two oligonucleotide primers (forward N-3 and reverse C-2) were designed based on the partial aminoterminal sequence of Sm-hPAF (9). Mixed oligonucleotide-primed (MOP)-PCR consisted of 30 cycles of denaturation at 94 °C for 30 s, annealing at 50 °C for 30 s, and extension at 72 °C for 15 s using the GeneAmp PCR system 9700 (Applied Biosystems, Foster City, CA, USA). The PCR product was resolved by 8% PAGE, and a single 41-bp product was amplified and cloned into *Escherichia coli* strain JM109 and sequenced (ABI 373 DNA Sequencer; Applied Biosystems). This amplified fragment is referred to as *sm-65*.

Southern blotting

Two micrograms of chromosomal DNA was digested to completion with *Eco*RI, *Hind*III, and *Pst*I (TaKaRa Biomedicals, Kyoto, Japan) or combinations thereof. The products were resolved by 1.0% agarose gel electrophoresis and transferred to a Hybond-N^+ membrane (GE Healthcare UK Ltd., Buckinghamshire, UK). *Sm-65* (Table 1) and 222 TBq/mmol of [α-P^{32}]-dCTP were mixed at a molar ratio of 1:10 and incubated at 37 °C for 1 h with terminal deoxynucleotidyl transferase (TaKaRa Biochemcals). [α-P^{32}]-dCTP was removed from the reaction mixture by Sephadex G-25 column (GE Healthcare UK Ltd.). Approximately 0.15 pmol of [α-P^{32}]-dCTP-labeled *sm-65* was as probe for Southern blotting. Southern blotting was carried out essentially as described by Sambrook et al. (13). The result of Southern blot hybridization revealed that the 2.5–3.5 kb DNA fragments with a strong hybridization signal contained the coding region of the *sm-hpaf* gene. Thus, the fragments were used in cassette PCR as the template.

Genomic mapping of *sm-hpaf*

The *sm-hpaf* gene was mapped by Southern hybridization and restriction analysis of cassette PCR-generated fragments using *Hind*III and *Pst*I. After complete digestion of each fragment, the products were resolved by 1.2% agarose gel electrophoresis, stained with ethidium bromide, and then the size of fragments was estimated from the photographs taken under the ultraviolet light.

Table 1. Nucleotide sequences of PCR primers and probes used in the study

Primer/Probe	Sequence
For the *sm-hpaf* gene cloning:	
Mixed oligonucleotide PCR forward N-3	5′-GAYGARCARGGIAAYCG-3′
Mixed oligonucleotide PCR reverse C-2	5′-GCIATRTTYCIGTYT-3′
Forward cas1 for 1st cassette PCR of signal peptide	5′-GTACATATTGTCGTTAGAACGCGTAATACGACTCA-3′
Forward cas2 for semi-nested PCR of signal peptide	5′-CGTTAGAACGCGTAATACGACTCACTATAGGGAGA-3′
Reverse cod1 for PCR of signal peptide	5′-GATGTTTTCGGTCTCAACTGGAC-3′
Forward cod3 for PCR of mature protein	5′-GTCCAGTTGAGACCGAAAACATCGC-3′
Reverse cas1 for 1st cassette PCR of mature protein	5′-GTACATATTGTCGTTAGAACGCGTAATACGACTCA-3′
Reverse cas2 for semi-nested PCR of mature protein	5′-CGTTAGAACGCGTAATACGACTCACTATAGGGAGA-3′
For Southern hybridization analysis:	
Sm-65	5′-GACGAGCAAGGGAATCGTCCAGTTGAGACCGAAAACATCGC-3′
For expression of the recombinant toxins:	
Forward *Sm-hpaf*	5′-GCGGATCCACAGAGCAAGGGAATCGTCC-3′
Reverse *Sm-hpaf*	5′-GCAAGCTTACTCATTCACAATTTTTTCATC-3′
Forward *sly*	5′-CGGGATCCCAAGATATTAATCAGTATTTTCAAAGC-3′
Reverse *sly*	5′-GCCAGCTGTTACTCTATCACCTCATCCGCA-3′

Cassette PCR

Ten micrograms of chromosomal DNA was digested with *Eco*RI and resolved by 1% agarose gel electrophoresis. The band containing 2.5–3.5 kb DNA fragments was excised, digested with 1 U β-agarase (TaKaRa Biochemicals), and the DNA was precipitated with ethanol. One microgram of DNA fragments was ligated with 10 pmol of *Eco*RI cassette (TaKaRa Biochemicals) using T4 DNA ligase at 16 °C for 16 h and the reaction product served as the cassette PCR template. Cassette PCR was performed in two directions using the TaKaRa LA PCR™ *in vitro* cloning kit and cassette primers (TaKaRa Biochemicals). Two primer pairs were designed to amplify the sequences encoding the signal peptide and the mature form of Sm-hPAF based on sequencing of the MOP-PCR product: forward cas 1 and reverse cod 1, and forward cod 3 and reverse cas 1, respectively (Table 1). Cassette PCR included 30 cycles of denaturation at 94 °C for 30 s, annealing at 60 °C for 90 s, and extension at 72 °C for 3 min. Both DNA amplicons were re-amplified in semi-nested PCR using two additional primer pairs: forward cas 2 and reverse cod 1 for the fragment encoding the signal peptide, and forward cod 3 and reverse cas 2 for the fragment encoding the mature protein (Table 1). Semi-nested PCR was performed using the reaction cycles described above. The nucleotide sequences were determined by direct sequencing of single PCR-amplified fragments in a DNA sequencer (ABI 373 DNA Sequencer; Applied Biosystems). The entire *sm-hpaf* gene was amplified by fusion cassette PCR using cassette PCR primer cas 2 and both products of cassette PCR obtained above. The amplified whole gene was cloned into plasmid pQE-9 (Qiagen GmbH, Hilden, Germany) and transformed into *E. coli* JM109.

Sequence data of the *sm-hpaf* gene

The sequence of the *sm-hpaf* gene revealed by genome walk was deposited in the data base (GenBank accession number AB051299) (14). The deposited sequence of the gene was also reviewed using PCR-direct sequencing of Nm-65 strain.

Preparation of recombinant Sm-hPAF and recombinant suilysin

Gene fragments encoding nSm-hPAF and native SLY (nSLY) were amplified by PCR from the genomes of strain Nm-65 and strain GTC430 using

the following primer sets (Table 1): forward *sm-paf* and reverse *sm-hpaf*, and forward *sly* and reverse *sly*, respectively. The primers were synthesized according to the gene sequence data for Sm-hPAF (GenBank accession number AB051299) and SLY (GenBank accession number AF043556). PCR was carried out in a 50-μL reaction mixture containing 0.01–0.1 μg genomic DNA, 10 pmol of each primer, 1 U of Pyrobest or Prime STAR HS DNA polymerase (TaKaRa Biochemicals), 0.2 mM dNTP, and 5 μL 10× PCR buffer using a thermal cycler (PCR Express; Hybaid Co., London, UK or GeneAmp PCR System; Perkin Elmer Life and Analytical Sciences, Inc., Waltham, MA, USA). Following agarose gel electrophoresis, the purified *sm-hpaf* and *sly* amplicons were digested with *Bam*HI/*Hind*III and *Bam*HI/*Pvu*II, respectively. The *sm-hpaf* and *sly* gene fragments ligated into pQE-9 (Qiagen GmbH) and pUHE1Δfd N-his s32 (a plasmid constructed by substitution of the segment carrying *cm*^{r} between the *Eco*RI and *Xba*I sites of pUHE21-2fdΔ12 (15) with the segment carrying the*σ32* gene between the *Eco*RI and *Nhe*I sites of pUHE212-1 s32 (16). JM109 cells competent for Sm-hPAF expression and Rosetta strains competent for SLY expression (Novagen, Merck KGaA, Damstadt, Germany) were transformed with each recombinant vector and selected on LB/ampicillin plates. Recombinant clones carrying the expression plasmid with the correct *sm-hpaf* and *sly* sequences were used in the following step.

Expression of mature forms of Sm-hPAF and SLY was induced by isopropyl-D-thiogalacto-pyranoside (Wako Pure Chemicals Co.). Collected cells were disrupted by sonication using the Astrason XL2020 (MISONIX, Inc., Farmingdale, NY, USA) and resuspended in 50 mM sodium phosphate buffer (PB, pH 8.0) containing 10 mM $MgCl_2$. Crude extracts were applied to a Ni-NTA affinity column (Qiagen GmbH) equilibrated with 50 mM PB (pH 8.0 for Sm-hPAF, pH 7.0 for SLY) containing 300 mM NaCl and eluted using an imidazole linear gradient (0–250 mM in PB) using high pressure liquid chromatography (Bio-Rad BioLogic, Cambridge, MA, USA). For further purification of rSm-hPAF, the fraction containing Sm-hPAF eluted from the Ni-NTA affinity column was diluted in 5 mM PB (pH 7.0), applied to a HiTrap SP HP-column (GE Healthcare UK Ltd.) equilibrated with 50 mM PB (pH 7.0), and eluted using a NaCl linear gradient (0–1 M in equilibration buffer). The fractions containing purified rSm-hPAF or rSLY were identified by immunoblotting, combined, and dialyzed against an approximately 100-fold volume of phosphate-buffered saline (PBS) at 4 °C 3–6 times to change the buffer to PBS. The protein concentration of each toxin solution was determined using the Bio-Rad Protein Assay kit (Bio-Rad Laboratories Inc., Hercules, CA, USA) and the solutions were stored at −80 °C until use.

Sequence analysis

Homology analyses for the gene and protein were performed using BLAST (NCBI) and Genetyx (Genetyx Corp., Tokyo, Japan); the sequences of the Sm-hPAF gene and protein and those of any homologs were aligned using ClustalX (EMBL). Structural comparisons were carried out by computer simulation using the HOMOLOGY module of Insight-II-Discover (Accelrys Inc., San Diego, CA, USA) based on the crystal data of perfringolysin O (PFO; PDB# 1PFO) and intermedilysin (ILY; PDB# 1S3R). The DNA sequences of the following homolog toxins were also used: AB029317 (ILY), AF043556 (suilysin, SLY), AY818308 (thuringiolysin), AY818309 (cereolysin O), D16824 (equisimilisin 0), D16825 (canilysin O), EF066515 (mitilysin MLY), EU597013 (lectinolysin, LLY), EU522486 (vaginolysin, VLY), M18638 (streptolysin O, SLO), M29030 (listeriolysin O, LLO), M36704 (PFO), M62709 (alveolysin, ALV), NX004557 (tetanolysin O), U84782 (pyolysin, PLO), NX010382 (sphaeriocolysin), X52474 (pneumolysin, PLY), X60461 (ivanolysin O), and X60462 (seeligeriolysin O). Phylogenetic analysis of *sm-hpaf* based on the maximum likelihood method was performed using DNAML from the PHYLIP software pack (J. Felsenstein, University of Washington).

Platelet aggregation

Human platelet-rich plasma (PRP) was obtained from a single adult female donor (YT, a colleague involved in this study) throughout the study. The aggregation reaction was carried out as described previously (7). Briefly, 200 μL PRP was mixed with 20 μL of various concentrations of test samples or reference toxin suspended in 10 mM PBS (pH 7.4), and the reaction mixture was incubated at 37 °C with stirring in a small tube. Platelet aggregation was measured using a four-channel aggregometer (Hema Tracer 601; Tokyo Kohden Co. Ltd., Tokyo, Japan) attached to a tracer (U 638; Nippon Denshi Kagaku Co. Ltd., Tokyo, Japan). The platelet count in PRP was 14.3 ± 0.85 (SD) × 10^4/mL. The aggregation potency of 1 mM adenosine 5′-diphosphate (ADP, the reference aggregation agent; Sigma Chemicals Co., St. Louis, MO, USA) in terms of light transmission after a 5-min reaction was set at 100%. Native PLY (nPLY) was kindly donated by Dr. J. C. Paton (University of Adelaide, South Australia). The following materials were also used as controls: the purified fraction obtained from cell lysates of empty vector pQE-9 transformant subjected to the same purification process used for rSm-hPAF (protein conc.: not detected); the supernatant obtained from sonicated cell lysates of the empty vector transformant (protein conc.: 2.95 mg/mL); the supernatant obtained from sonicated cell lysates of rSm-hPAF-expressing *E. coli* (protein conc.: 1.09 mg/mL);

and lipopolysaccharide (1 mg/mL, *E. coli*, O111:B4; Difco Laboratories, Detroit, MI, USA).

Hemolytic activity

Each mixture of 500 μL Dulbecco's PBS (without Mg^{2+} and Ca^{2+}) containing various amounts of rSm-hPAF or rSLY and 0.5% (v/v) human, horse, rabbit, rat, or chicken erythrocytes was incubated for 1 h at 37 °C in a microcentrifuge tube. After centrifugation (800 *g* for 5 min at 4 °C), each 200 μL supernatant was transferred to one well of a 96-well microtiter plate and absorbance at 540 nm was measured in a microplate reader Model 550 (Bio-Rad).

Immunoblotting

rSm-hPAF was resolved by SDS-PAGE (17). One portion of the gel was stained with Coomassie brilliant blue R250 (Sigma Chemical Co.) and the proteins in the second portion were transferred to a nitrocellulose membrane (SSBA85; Schleicher & Schuell Co., Dassel, Germany) under constant current (1 A) for 1 h, as described previously (18). The membrane was probed with either mouse anti-Sm-hPAF monoclonal antibody (mAb NOT-12, see below) or mouse anti-hisTag mAb (mAb hisTag; Qiagen). After incubation for 2 h, alkaline phosphatase-labeled goat anti-mouse IgG antibody (Cappel Laboratories, Cochranville, PA, USA) was applied to the membrane and incubated for 1 h at room temperature. The reaction was developed by addition of enzyme substrate solution, which consisted of Tris-HCl buffer (pH 10.0) containing 3 mM $MgCl_2$, 0.1% (w/v) nitroblue tetrazolium (Sigma Chemical Co.) in distilled water, and anhydrous dimethylformamide (Piece Chemical Co., Rockford, IL, USA) (19).

Production of monoclonal antibodies to Sm-hPAF

BALB/c mice were given an initial intraperitoneal injection of 250 μg of the extracellular products (ECP) of strain Nm-65 emulsified in Freund's incomplete adjuvant (FICA; Difco Laboratories). The mice then received 250 μg ECP with FICA by intraperitoneal injection each week for 4 weeks. Following the final injection, they received an intravenous injection of 500 μg ECP alone. Three days later, spleen cells were removed and spleen cell-myeloma cell (NS-1) hybrids were prepared with a purified nSm-hPAF preparation (9, 18). The monoclonal antibodies in the supernatants of hybridoma cells were assayed using enzyme-linked immnosorbent assay (18). We screened 60 hybridoma clones: the supernatants obtained from seven clones were reacted with nS-hPAF. All seven positive clones were established after cloning twice by the limiting dilution method. The supernatant obtained from one of the seven clones was used as mAb in this study. The mAb was designated as NOT 12 and immunoglobulin (Ig) subclasses of mAb NOT 12 were determined by double immunodiffusion techniques using commercially prepared subclass-specific antisera (Serotec Ltd., Bicester, UK). The mAb NOT-12 formed a clear precipitin line with anti-IgG2a antibody (subclass IgG2a).

Release of lactate dehydrogenase

Platelet-rich plasma specimens (200 μL) were incubated with 20 μL of each test toxin at 37 °C. After 5 min, the tubes were centrifuged at 650 *g* for 15 min and lactate dehydrogenase (LDH) activity in the supernatants was determined using an automated analyzer (BioMajesty, JCA-BM9030; Japan Electron Optics Laboratory, Ltd., Tokyo, Japan) and a PUREAUTO S LD diagnostic kit (Daiichi Pure Chemicals Co., Ltd., Tokyo, Japan). Non-stimulated cells were disrupted by three cycles of freezing (−80 °C) and thawing (23 °C) and the total amount of LDH in the cells was measured as a positive control. All assays were performed in triplicate.

Light and transmission electron microscopy

Platelets treated with rSm-hPAF were fixed in 2.5% glutaraldehyde in 0.1 M PB (pH 7.4) overnight at room temperature. The samples were post-fixed with 1% osmium tetroxide in the same buffer for 1 h, dehydrated through a graded-ethanol series, and embedded in Epon 812 resin (Okenshoji Co. Ltd., Tokyo, Japan). Before ultra-thin sections were cut, semi-thin sections were stained with 0.1% toluidine blue and examined by light microscopy for morphological orientation. Ultra-thin sections were cut using a Leica Ultracut R ultramicrotome (Leica, Mikrosysteme, Wien, Austria) with a diamond knife (Diamond Ltd., Basel, Switzerland) and stained with routine electron staining of 4% uranyl acetate in distilled water and 2.7% lead citrate (20). The sections were observed at 80 kV under an H-7500 electron microscope (Hitachi High-Technologies Corp., Tokyo, Japan).

Statistical analysis

Analysis of variance was calculated using the Bonferroni method. The calculation was carried out using Microsoft Office Excel 2007 (Microsoft Corp., Tokyo, Japan).

RESULTS

Deduced amino acid sequence of Sm-hPAF

The complete amino acid sequence of Sm-hPAF produced by strain Nm-65 was deduced from the

DNA sequence (Fig. 1A). The primary structure of rSm-hPAF was aligned with VLY, ILY, PLY, MLY, SLY, and lectinolysin (LLY) (21) (Fig. 1A). The native mature form of rSm-hPAF consisted of 629 amino acid residues; no cysteine residues occurred in the mature protein. The 162

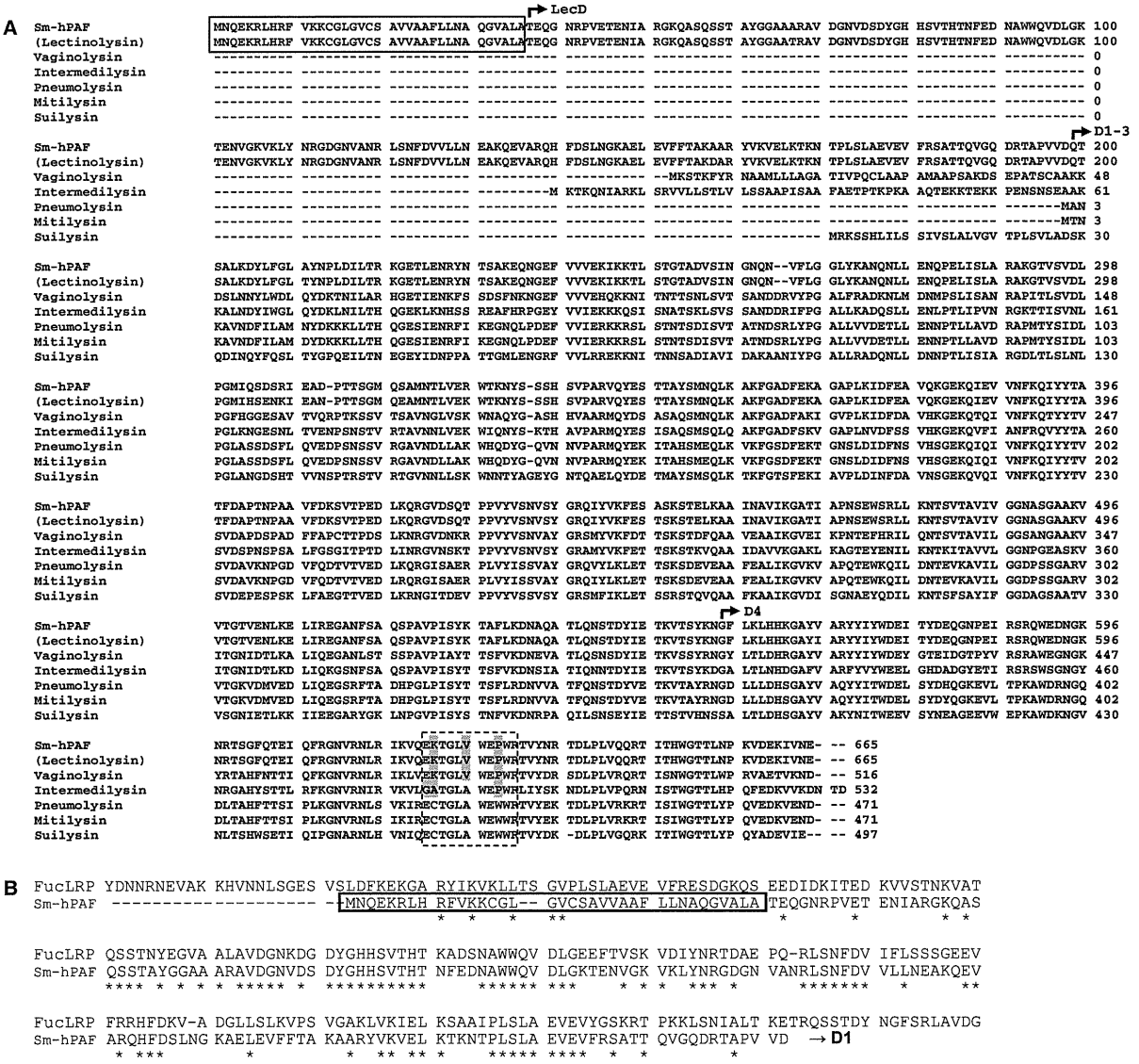

Fig. 1. Sequence alignments of recombinant *Streptococcus mitis*-derived human platelet aggregation factor (rSm-hPAF) and homologous proteins. (A) Sequence alignment of rSm-hPAF (strain Nm-65), lectinolysin (strain SK598), vaginolysin (strain 14018), intermedilysin (strain UNS46), pneumolysin (strain NCTC7466), mitilysin (strain COL15), and suilysin (strain 1933). Open boxes indicate the signal peptides of Sm-hPAF. Arrows denote the top of each domain. rSm-hPAF precursor includes 665 amino acid residues: the signal peptide, M1-A36; fucolectin-related protein domain (Lec domain), T37-D198; domains 1–3, Q199-N554; and domain 4, G555-E665. The box with a broken line represents the undecapeptide region. rSm-hPAF possesses three substitutions, indicated by shaded letters, in the consensus sequence of common cholesterol-dependent cytolysins: ECTGLAWEWWR. (B) Alignment of the signal peptide/fucolectin-related protein domain of Sm-hPAF and Y691-G928 of the pneumococcal fucolectin-related protein (FucLRP, GenBank accession no. CP000410.1). The box with a solid line indicates the signal peptide of Sm-hPAF. The 162 amino-terminal residues of Sm-hPAF show high homology (47.5% identity) with this region of FucLRP.

amino-terminal residues of Sm-hPAF protein were homologous to a segment of the pneumococcal fucolectin-related protein (Fig. 1B).

The sequence of the *sm-hpaf* gene cloned by genomic walk was compared with the result of PCR-direct sequencing of whole *sm-hpaf* gene. Review of the *sm-hpaf* gene revealed that the correct sequence of the position 138 in ORF of the gene was A (ACA) corresponding to the position 390 of the deposited sequence (AB051299): C (ACC), although there was no change in coded amino acid level, Thr.

Partial characterization of rSm-hPAF

SDS-PAGE of nSm-hPAF, rSm-hPAF, and rSLY is shown in Fig. 2A. The molecular weight of nSm-hPAF on SDS-PAGE was around 66 kDa; as rSm-hPAF was labeled with an amino-terminal extrapeptide (MRGSH HHHHHGS) including the hexaHisTag, the molecular weight of rSm-hPAF was approximately 70 kDa on SDS-PAGE. The molecular weight of rSLY was approximately 57 kDa on SDS-PAGE. rSm-hPAF reacted with mAb NOT-12 and anti-pentaHisTag mAbs in immunoanalysis (Fig. 2B), while mAb NOT-12 did not react with rSLY (data not shown).

The molecular weight and isoelectric point of mature rSm-hPAF was calculated to be 69 784 kDa and 8.76, respectively. Two cysteine residues were detected in the signal peptide region (Fig. 1A), but cysteine was not predicted to appear in the mature rSm-hPAF. There were no substantial differences between nSm-hPAF (9) and rSm-hPAF in terms of molecular weight, isoelectric point, and cysteine residue content.

The addition of 0.1 μg/mL rSm-hPAF to human, horse, rabbit, rat, and chicken erythrocytes induced almost 100% hemolysis within 15 min (Fig. 3). The hemolytic activity of ILY was strictly human specific, as shown previously (22); however, neither rSm-hPAF nor rSLY exhibited strictly human-specific activity. Hemolytic activity was also eliminated by heat denaturation (at 96 °C for 10 min) of rSm-hPAF and rSLY (Fig. 3A,B, asterisks). Moreover, the fraction obtained from transformants with empty expression vectors, pQE-9 and pUHE 1Δfd n-his s32, also showed no hemolytic activities (data not shown). Platelet aggregation

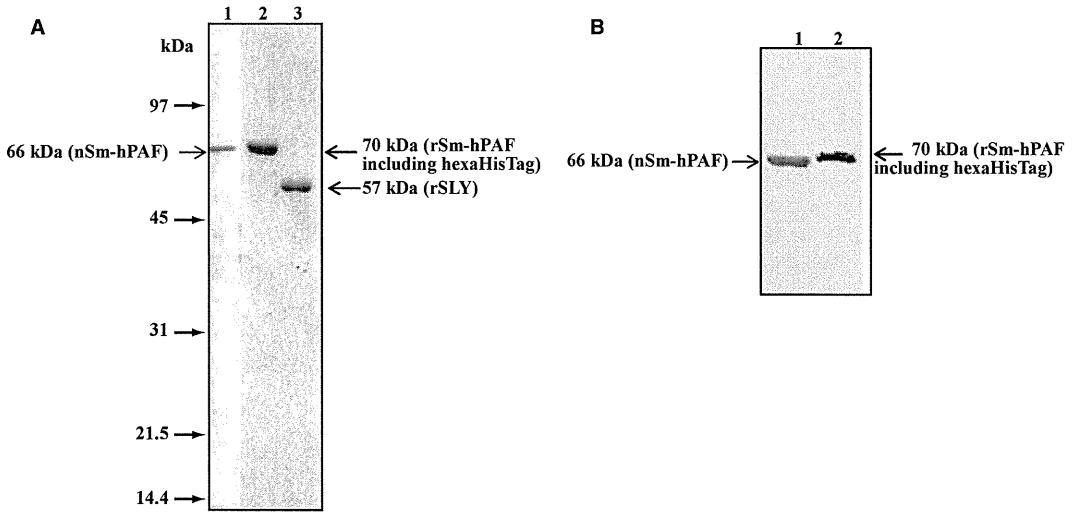

Fig. 2. Protein profiles of native *Streptococcus mitis*-derived human platelet aggregation factor (Sm-hPAF), recombinant Sm-hPAF (rSm-hPAF), and recombinant suilysin. (A) SDS-PAGE profiles. Lane 1; nSm-hPAF (mw; approximately 66 kDa), lane 2; rSm-hPAF including hexaHisTag (mw; approximately 70 kDa), lane3; rSLY (mw; approximately 57 kDa). Molecular weight markers appear to the left of lane 1. (B) Immunoblot profiles of rSm-hPAF incubated with mAb NOT-12 (lane 1, mw; approximately 66 kDa) and anti-pentaHisTag monoclonal antibodies (lane 2, mw; approximately 70 kDa).

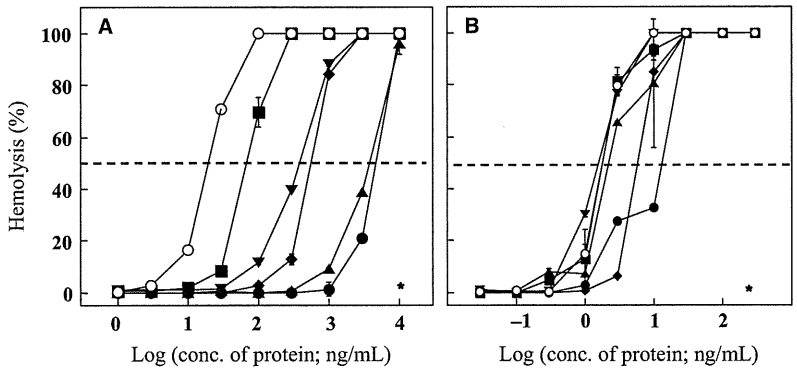

Fig. 3. Hemolytic activity of recombinant *Streptococcus mitis*-derived human platelet aggregation factor (rSm-hPAF) and recombinant suilysin in various animal erythrocytes. (A) rSm-hPAF. (B) rSLY. Human (open circle), horse (square), rabbit (turned triangle), rat (diamond), sheep (triangle), and chicken (closed circle) erythrocytes were assayed. The hemolysis assay was carried out as described in Materials and methods, and the results from triplicated measurements are shown. Asterisks, rSm-hPAF and rSLY treated at 96 °C for 10 min.

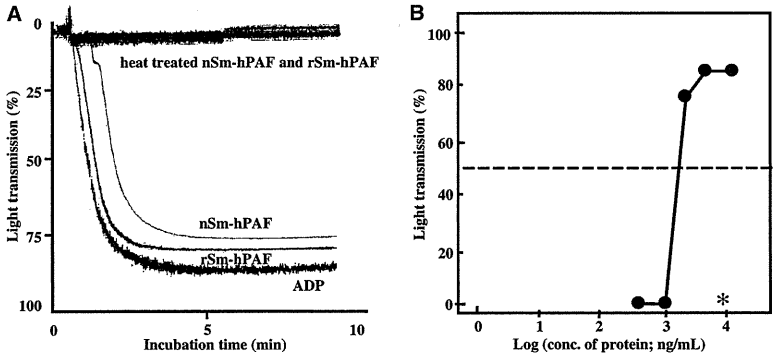

Fig. 4. Analysis of human platelet aggregation resulting from recombinant *Streptococcus mitis*-derived human platelet aggregation factor (rSm-hPAF). (A) Patterns of human blood platelet aggregation induced by native Sm-hPAF (nSm-hPAF) and recombinant Sm-hPAF (rSm-hPAF). Aggregation of a reaction mixture consisting of 200 μL of PRP and 20 μL of toxin, nSm-hPAF, or rSm-hPAF (containing 15 μg/mL protein) was determined using aggregometer; 1 mM ADP served as the reference aggregation agent. Both nSm-hPAF and rSm-hPAF were treated at 60 °C for 10 min. (B) A reaction mixture consisting of 200 μL of PRP and 20 μL of rSm-hPAF (0.1–10 μg protein/mL). The concentration of protein was expressed as log value. The potency of ADP in terms of increased light transmission due to platelet aggregation after 5 min reaction was taken as 100% and the potency (%) of rSm-hPAF was determined by comparing with that of ADP. Asterisk, heat treated rSm-hPAF.

caused by rSm-hPAF was essentially identical to that caused by nSm-hPAF (Fig. 4A). The lag time, speed, and extent of the aggregation were dependent on the concentration of rSm-hPAF; the aggregation induced by 15, 5, and 3 μg/mL rSm-hPAF was 70%, 70%, and 60%, respectively, relative to ADP aggregation activity (Fig. 4B). Both rSLY and PLY also exhibited human platelet aggregation activity (Fig. 5A,B). The platelet aggregation activities of nS-hPAF, rSm-hPAF, rSLY, and PLY, respectively were eliminated by heat treatment at 60 °C for 10 min (Figs 4 and 5). The following materials did not react with human platelets (Fig. 6): the purified fraction obtained from cell lysates of empty-vector (pQE-9) transformant subjected to the same purification process used for rSm-hPAF; the supernatant obtained from sonicated cell lysates of empty-vector (pQE-9) transformant; and lipopolysaccharide (Fig. 6C). Two preparations, rSm-hPAF and the supernatant obtained from sonicated cell lysates of rSm-hPAF-expressing *E. coli*, reacted with human platelets (Fig. 6A,B).

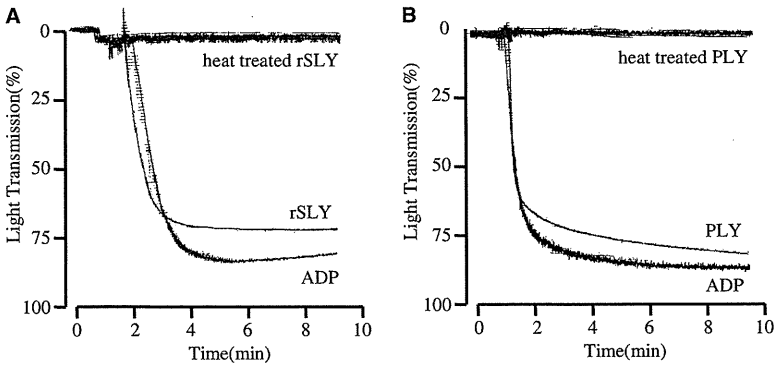

Fig. 5. Human blood platelet aggregation patterns of other CDCs. (A) rSLY. (B) PLY. The reaction mixture consisted of 200 μL of PRP and 20 μL of each toxin solution. The protein concentration of each toxin solution is shown in Table 2. Aggregation was determined using aggregometer; 1 mM ADP was the reference aggregation agent. Each toxin treated at 60 °C for 10 min was also assayed.

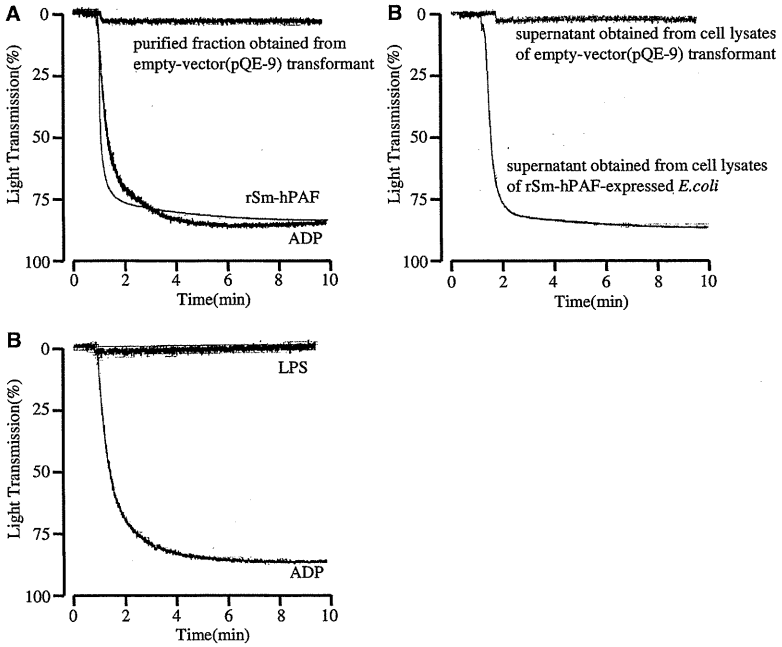

Fig. 6. Confirmation of the effect of impurity in recombinant *Streptococcus mitis*-derived human platelet aggregation factor (rSm-hPAF) fraction from *Escherichia coli* on human blood platelet aggregation activity. (A) rSm-hPAF and the purified fraction obtained from empty vector pQE-9-transformant subjected to the same purification process used for rSm-hPAF (protein conc.: not detected). (B) The supernatant obtained from sonicated cell lysates of empty-vector pQE-9-transformant (protein conc.: 2.95/mL) and of rSm-hPAF-expressing transformant (protein conc.: 1.09 mg/mL). (C) Lipopolysaccharide (1 mg/mL). Aggregation was determined using aggregometer; 1 mM ADP was used as the reference aggregation agent.

Homology analysis

The amino acid sequence from residue 199 to the end of the rSm-hPAF molecule was highly homologous to the sequences of various hemolytic toxins classified into the CDCs produced by Gram-positive bacteria (Fig. 1A). Maximum-likelihood phylogenic analysis of *sm-hpaf* indicated that Sm-hPAF belongs to the CDC family, along with PLY, SLY, ILY, and MLY. MLY is secreted from several *S. mitis* strains (23). Remarkable identity was found CDC such

as VLY (56.8%) produced by *Gardnerella vaginalis* (24), ILY (55%), PLY (51.4%), MLY (51.6%), SLY (45.3%), ALY (39.7%), PFO (38.9%), LLO (38.0%), PLO (37.8%), and SLO (36.3%).

A phylogenetic tree of the CDCs appears in Fig. 7. Sm-hPAF was classified into the same cluster as ILY, LLY, MLY, PLY, SLY, and VLY, but was only distantly related to SLO, PFO, and LLO. Recently, Farrand et al. (21) reported that LLY, the molecule derived from *S. mitis* strain SK597, was almost the same as the molecular sequences of Sm-hPAF (Fig. 1A).

Although there are differences in amino acid sequence between PLY and MLY, they occur only at 13 amino acid positions; however, the amino acid sequence of rSm-hPAF is remarkably different from those of PLY, MLY, ILY, and SLY (Fig. 1A). Crystal structural and computer simulation analyses divided these molecules into four domains (domains 1–4) (25–27). According to molecular modeling, rSm-hPAF has a similar basic structure and four domains, but the region from the amino terminus to amino acid 162 was not found in VLY, ILY, PLY, MLY, or SLY (Fig. 1A). Significant homology was detected between the amino-terminal 162 amino acid residues of Sm-hPAF, LLY, and a pneumococcal fucolectin-related protein (Fig. 1B), suggesting that *sm-hpaf* may be the product of gene fusion (28).

It has been predicted that the undecapeptide present in domain 4 of CDCs may interact with cholesterol on erythrocyte membranes (15, 29). The conserved undecapeptide region of CDCs was altered from ECTGLAWEWWR in PLY, MLY, and SLY and from GATGLAWEPWR in ILY to EKTGLVWEPWR in Sm-hPAF, LLY, and VLY (boxed, Fig. 1A).

Platelet aggregation by cholesterol-dependent cytolysins

rSLY and PLY of CDCs induced human platelet aggregation as strongly as rSm-hPAF; a lag phase of 1.5–2 min was followed by definite aggregation and aggregation was nearly maximal after 4–5 min (Figs 4 and 5). Aggregation

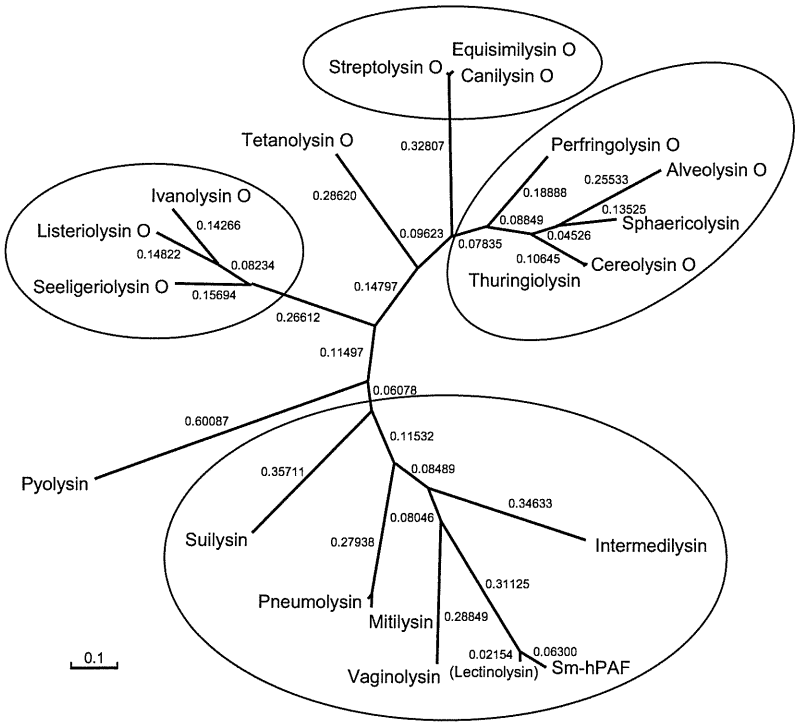

Fig. 7. Phylogenetic analysis of the cholesterol-dependent cytolysins. Phylogenetic analysis of *sm-hpaf* based on the maximum likelihood method was performed using DNAML from the PHYLIP software package. Number is branch length and the bar shows a scale of branch length.

activity of rSm-hPAF, rSLY, and PLY was inactivated by heat treatment at 60 °C for 5 min (Figs 4 and 5). Both of rSm-hPAF and the supernatant obtained from sonicated cell lysates of rSm-hPAF-expressing *E. coli* reacted with human platelets; however, none of the supernatant obtained from sonicated cell lysates or the purified fraction of empty-vector pQE-9-transformant – which were obtained by the same purification process used for rSm-hPAF – reacted with human platelets (Fig. 6A,B). Lipopolysaccharide also did not react with human platelets (Fig. 6C).

Table 2 reports the aggregation activities of each CDC species relative to ADP activity. There were marked differences in the concentrations of CDCs required to yield maximum aggregation (defined as 60–82% aggregation rate), indicating that the aggregation activity was toxin dependent.

LDH release from platelets aggregated by cholesterol-dependent cytolysins

Lactate dehydrogenase assays were performed to determine whether the hemolytic toxins caused platelet lysis (Table 2). The amount of LDH released from positive control cells was 646.5 ± 14.8 IU/L and the spontaneous release of LDH in supernatant fluids from non-stimulated platelets (negative control) was 120 ± 2.8 IU/L. When the amount of LDH released from the positive control cells was set equal to 100%, the LDH released into the supernatant by rSm-hPAF was 34.4 ± 2.52%; PLY, 20.5 ± 0.99%; rSLY, 23.4 ± 0.88%; ADP, 18.9 ± 0.21%; and negative control, 18.6 ± 0.43%. The amount of released LDH was not significantly different between negative control and toxins (PLY and rSLY), including ADP. However, a slight but significant difference was observed between the negative control and rSm-hPAF ($p < 0.05$). To a certain degree, the extent of aggregation and the amount of LDH released varied according to the sort of toxins and concentration.

Light and transmission electron microscopic observation of activated platelets

To confirm that the LDH release measured above was not the result of platelet lysis, we examined the morphology of platelets activated with rSm-hPAF, rSLY, and PLY by light and electron microscopy. Platelet aggregation was not observed following toluidine blue staining of semi-thin sections of non-stimulated platelets (Fig. 8A). Non-stimulated PRP was characterized by spindle-shaped cells (platelets) and round cells (monocytes and/or granulocytes; Fig. 8A). However, platelets stimulated with ADP, rSm-hPAF, rSLY, and PLY were aggregated (Fig. 8B–E), but platelet aggregation was not caused by the heat-treated toxins. Although LDH was slightly released from platelets stimulated with rSm-hPAF, platelet lysis was not observed by light microscopy. Similar results were obtained by electron microscopy of

Table 2. Percent aggregation and lactate dehydrogenase (LDH) release from platelets stimulated with cholesterol-dependent cytolysins

Toxin	Concentration (μg/mL)	Maximum % aggregation (relative % aggregation)	LDH release (IU/L ± SD) [Relative release (%)[4]]
rSm-hPAF	10.9	68 (82.0)	223 ± 16.3 (34.4 ± 2.52)[5]
PLY	30.0	60 (60.0)	132.5 ± 6.4 (20.5 ± 0.99)
rSLY	3.00	66 (81.3)	151 ± 5.7 (23.4 ± 0.88)
Adenosine 5′-diphosphate[1]	1 mM	80 (100)	122 ± 1.4 (18.9 ± 0.21)
Negative control[2]			120 ± 2.8 (18.6 ± 0.43)
Positive control[3]			646.5 ± 14.8 (100 ± 2.29)

[1]1 mM adenosine 5′-diphosphate served as the reference aggregation agent.
[2]The amount of LDH released from non-stimulated platelets.
[3]The total amount of LDH in the platelets disrupted by freezing and thawing.
[4]The amount of LDH released in response to each toxin relative to that released by the positive control.
[5]A slight but significant difference was observed between negative control and rSm-hPAF ($p < 0.05$).

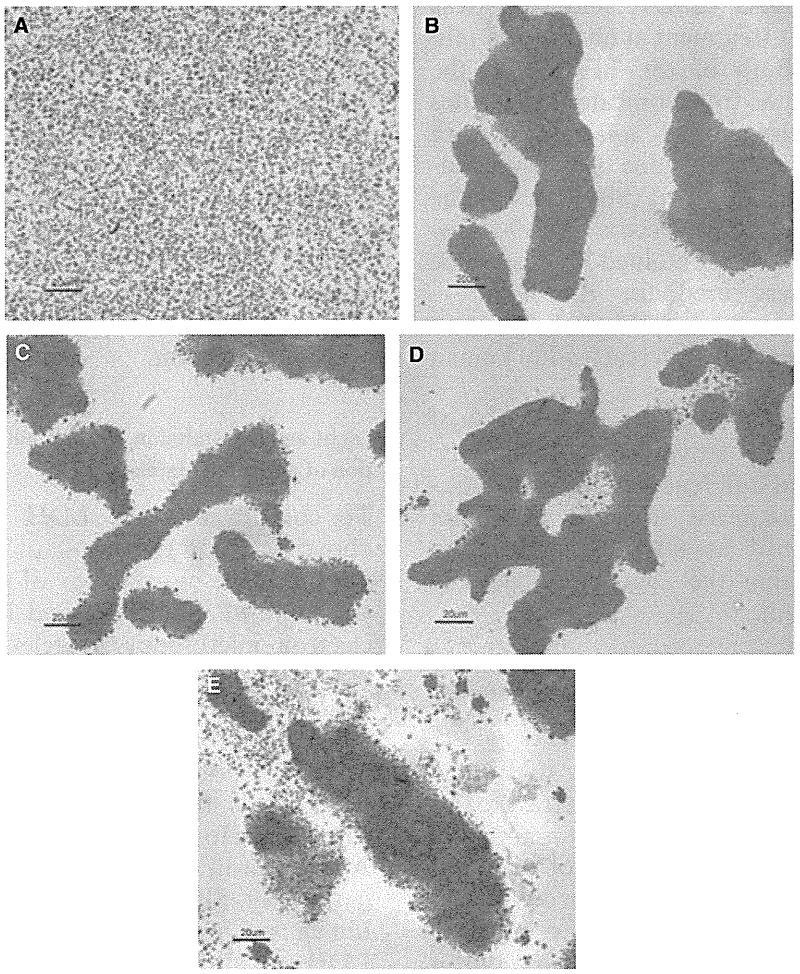

Fig. 8. Light microscopic observation of the effect of CDCs on human platelets. Semi-thin sections of platelet preparations were stained with toluidine blue. (A) Non-stimulated platelets. Spindle-shaped cells (platelets) and several round cells (monocytes and/or granulocytes) were abundant (×100). (B) 1 mM ADP-stimulated platelets (×400). (C) rSm-hPAF-stimulated platelets (×400). (D) rSLY-stimulated platelets (×400). (E) PLY-stimulated platelets (×400).

aggregated human platelets 5 min after stimulation with rSm-hPAF (Fig. 9). Non-stimulated human platelets contained many dense granules, mitochondria, the circumferential band of microtubules, the channels of the open canalicular system, and glycogen granules (Fig. 9A). In contrast, platelets stimulated with rSm-hPAF contained many pseudopodia (Fig. 9B) and many granules and the canalicular system disappeared without cell lysis. Furthermore, amorphous materials originating from granules were observed on the surface of activated platelets and closed vacuoles appeared from the canalicular system (Fig. 9B). Following stimulation with rSm-hPAF, thrombi were often formed and intact platelets involved in the thrombus were observed (Fig. 9C). Taken together, these data demonstrate that platelets were activated with rSm-hPAF and platelet lysis was not observed by light or electron microscopy.

DISCUSSION

Previously, we demonstrated that the concentrated culture supernatant of *S. mitis* strain Nm-65 was a powerful inducer of platelet aggregation (9). In a preliminary study, we found that all PRP specimens obtained from KD patients reacted with Sm-hPAF. However, the studies

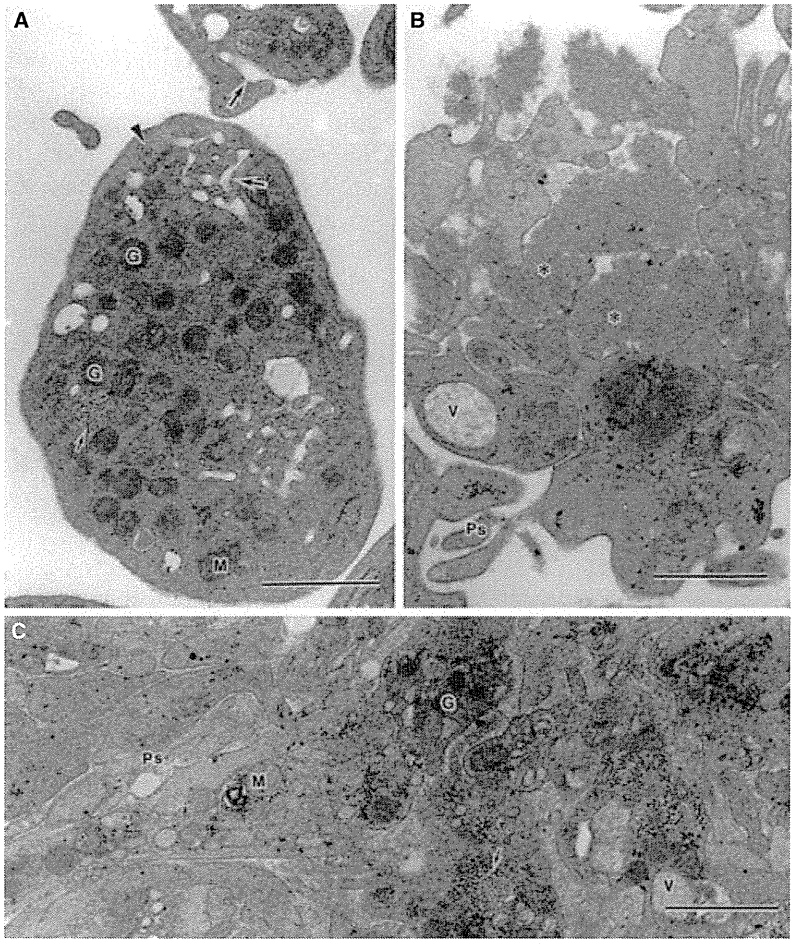

Fig. 9. Transmission electron microscopic observation of the effect of recombinant *Streptococcus mitis*-derived human platelet aggregation factor (rSm-hPAF) on human platelets. (A) Non-stimulated human platelets contained many dense granules. (B) Platelets stimulated with rSm-hPAF (9.4 μg/mL) were aggregated and many pseudopodia were visible. Many granules and the canalicular system disappeared without cell lysis; amorphous materials that originated from granules were observed on the surface of activated platelets. (C) Stimulation with rSm-hPAF induced thrombus formation in some cases; intact platelets involved in the thrombus are visible. G, granules; M, mitochondria; Ps, pseudopodia; V, vacuoles; asterisks, amorphous materials (secreted from granules); arrowhead, circumferential band of microtubules; arrows, surface-connected canalicular system; arrows, glycogen granule. Scale bar represents 1 μm.

also showed considerable individual differences between non-KD patients (other febrile diseases) and healthy adults with respect to the susceptibility of PRP specimens to aggregation by Sm-hPAF (9). As platelet aggregation factor-producing *S. mitis* have been isolated from the oral cavities of non-KD patients (7), it is not clear whether Sm-hPAF-producing strains are involved in the pathogenesis of KD.

Here we have determined the complete sequence of *sm-hpaf*, including 252 bases upstream and 98 bases downstream of the open reading frame, which encoded a 665-amino acid protein, including the signal sequence (Fig. 1A).

The mature form of Sm-hPAF was expressed in *E. coli* JM109 as a His-tagged protein (rSm-hPAF); no substantial difference in its molecular weight, isoelectric point, and biological activities with nSm-hPAF (9). Although there were two cysteine residues in the signal peptide region (Fig. 1A), there were no cysteines in the mature Sm-hPAF.

Generally, CDC molecules are divided into four domains (25–27); however, rSm-hPAF

possesses an additional 162 amino acid residues that are not found in other CDC molecules, except for LLY (21). This domain is homologous to a portion of the pneumococcal fucolectin-related protein (Fig. 1B). It has been reported that the amino-terminal domain of an *S. mitis* (strain SK597)-derived CDC (LLY) is homologous to the pneumococcal fucolectin-related protein, and this domain (Lec domain) reacts specifically with difucosylated glycans within Lewis b and y antigens and release calcein in a pore-dependent fashion from calcein-loaded PRP (21). LLY does not induce platelet aggregation despite increasing light transmission (as measured by aggregometer). Although rSm-hPAF has Lec domain at the amino terminus LLY, rSm-hPAF does induce platelet aggregation as shown in this work. On the other hand, PLY and rSLY, which do not have Lec domains, also induced platelet aggregation. Therefore, the site of platelet aggregation action in the molecule of CDCs, such as rSm-hPAF, PLY, and SLY, is likely to be located in domains 1–4 and the amino-terminal Lec domain has far less or no participation in this action.

It is possible that the entire *sm-hpaf* gene derives from a horizontal gene transfer between *S. mitis* and other bacteria, including *S. pneumoniae* and the viridans group of the oral streptococci (28). It is well established that these streptococcal group have an effective competence-stimulating system, ComCDE, which enables gene exchange among bacteria (30). The sequence of the undecapeptide in the carboxyl-terminal region of rSm-hPAF is the same as those of VLY (24) and LLY (21). On the other hand, there are considerable differences in amino acid sequence between rSm-hPAF and the CDCs, such as PLY, MLY, and ILY, especially in the undecapeptide sequence (Fig. 1A). The undecapeptide region is thought to be important for toxin-cholesterol/cell membrane interactions in ordinary CDCs such as PLY and PFO. Three amino acid residues, C, A, and the second W in the typical undecapeptide (ECTGLAWEWWR) found in PLY, MLY, and SLY, are replaced by K, V, and P in the rSm-hPAF molecule. Three amino acid residues, G, A, and the second A in the undecapeptide found in the ILY, are replaced by E, K, and V in the Sm-hPAF. The amino acid sequence of VLY is 56.8% identical to rSm-hAF and its undecapeptide sequence is identical to Sm-hPAF, but differs from ILY (Fig. 1A). Both VLY and ILY lyse human erythrocytes in a species-specific manner and both interact with the complement regulatory molecule (human CD59) on target cells (22, 24, 30). Because the lytic activity of rSm-hPAF toward erythrocytes is not human specific, it is likely that a complicated multi-binding mechanism regulate the reactivity of Sm-hPAF toward erythrocytes. Further investigation is required to understand how the rSm-hPAF undecapeptide region interacts with cholesterol-rich membranes and why species specificity varies among ILY, VLY, and Sm-hPAF. We are also interested in determining whether VLY and ILY aggregate human platelets.

The aggregation activity was inactivated by heat treatment (60 °C for 10 min) of rSm-hPAF, rSLY, and PLY. The supernatant obtained from sonicated cell lysates of empty vector pQE-9- transformant by sonication and *E. coli* LPS did not activate PRP. These results showed that the platelet aggregation activity of rSm-hPAF is not due to contamination with cellular components derived from expression system using *E. coli* cells.

Not the LDH assays, but the microscopic observation was carried out to investigate the platelet lysis by CDCs. Although a slight but significant difference was observed between negative control and rSm-hPAF ($p < 0.05$) in LDH assay, the lysis of platelets was not observed on light microscopy. Light microscopy also clearly showed platelet aggregation following stimulation with rSm-hPAF, PLY, and rSLY (Fig. 8C–E), but not in non-stimulated platelets (Fig. 8A). Electron microscopy indicated that deposits within platelet granules were released after stimulation with rSm-hPAF, that platelet aggregation occurred, and that thrombi were formed, indicating that platelets were not lysed by rSm-hPAF (Fig. 9).

It was suggested that the susceptibility of PRP specimens to the aggregation by Sm-hPAF differed among individuals; the patterns of platelet aggregation induced by Sm-hPAF may be divided into three groups: non-aggregation, low-aggregation, and aggregation (9). Our preliminary study suggested that the presence of an inhibitory factor against Sm-hPAF in the plasma from a non-aggregated donor (9).

The reason for the discrepancy between our results and those of Farrand et al. (21) requires further investigation. Our results also suggest that the platelet-binding site responsible for platelet aggregation on Sm-hPAF is not located within the amino-terminal Lec domain, because this domain does not exist in PLY and SLY molecules which can induce the platelet aggregation (Fig. 1A). Investigations of the binding site(s) and mode of action of Sm-hPAF to erythrocytes and platelet membranes are currently in progress.

We are grateful to Dr. James C. Paton, University of Adelaide, for providing pneumolysin. We also thank Dr. S. Sato, Nippon Medical School, for help with transmission electron microscopy. This work was supported in part by grants to H.O. and H.N. from the Ministry of Education, Science, and Culture of Japan.

REFERENCES

1. Evans AS. Discussion of etiology. In: Shulman S, editor. Kawasaki Disease. New York, NY, USA: Alan R. Liss Inc., 1987: 141–4.
2. Furukawa S, Matsubara T, Jujoh K, Yone K, Sugawara T, Sasai K, et al. Peripheral blood monocyte/macrophages and serum tumor necrosis factor in Kawasaki disease. Clin Immunol Immunopathol 1988;48:247–51.
3. Matsushita K, Fujimaki W, Kato H, Uchiyama T, Igarashi H, Ohkuni H, et al. Immunopathological activities of extracellular products of Streptococcus mitis, particularly a superantigenic fraction. Infect Immun 1995;63:785–93.
4. Takada H, Kawabata Y, Tamura M, Matsushita K, Igarashi H, Ohkuni H, et al. Cytokine induction by extracellular products of oral viridans group streptococci. Infect Immun 1993;61:5252–60.
5. Yanagawa I. Epidemiology of Kawasaki disease in Japan. In: Shulman S, editor. Kawasaki Disease. New York, NY, USA: Alan R. Liss Inc., 1987: 5–17.
6. Yanagawa I. Epidemiological pictures of Kawasaki disease in Japan. In: Takahashi M, Taubert K, editors. Proceeding of the Fourth International Symposium on Kawasaki Disease. Dallas, TX, USA: Am. Heart Assoc., 1993: 1–9.
7. Ohkuni H, Todome Y, Mizuse M, Ohtani N, Suzuki H, Igarashi H, et al. Biologically active extracellular products of oral viridans streptococci and the aetiology of Kawasaki disease. J Med Microbiol 1993;39:352–62.
8. Kawamura Y, Whiley RA, Shu S-E, Ezaki T, Hardie JM. Genetic approaches to the identification of the mitis group within the genus Streptococcus. Microbiology 1999;145:2605–13.
9. Ohkuni H, Todome Y, Okibayashi F, Watanabe Y, Ohtani N, Ishikawa T, et al. Purification and partial characterization of a novel human platelet aggregation factor in the extracellular products of Streptococcus mitis, strain Nm-65. FEMS Immunol Med Microbiol 1997;17:121–9.
10. Tweten RK. Cholesterol-dependent cytolysins, a family of versatile pore-forming toxins. Infect Immun 2005;73:6199–209.
11. Alouf JE. Molecular features of the cytolytic pore-forming bacterial protein toxins. Folia Microbiol 2003;48:5–16.
12. O'Connor SP, Cleary PP. In vivo Streptococcus pyogenes C5a peptidase activity; analysis using transposon- and nitrosoguanidine-induced mutants. J Infect Dis 1987;156:495–504.
13. Sambrook J, Fritsh EF, Maniatis T. Analysis of genomic DNA by Southern hybridization in molecular cloning. In: Sambrook J, Fritsh EF, Maniatis T, editors. A Laboratory Manual. New York, NY, USA: Cold Spring Laboratory Press, 1989: 9.31–.57.
14. Watanabe Y, Ohkuni H. Human platelet aggregation factor produced by Streptococcus mitis. NCBI Sequence Viewer 2006; v2.0 (Published only in Database)
15. Tomoyasu T, Arsene F, Ogura T, Ogura T, Bukau B. The C terminus of sigma(32) is not essential for degradation by FtsH. J Bacteriol 2001; 183:5911–7.
16. Gamer J, Bujard H, Bukau B. Physical interaction between heat shock proteins DnaK, DnaJ, and GrpE and the bacterial heat shock transcription factor sigma 32. Cell 1992;69:833–42.
17. Laemmli UK. Cleavage of structural proteins during the assembly of the head of bacteriophage T4. Nature 1970;227:680–5.
18. Ohkuni H, Todome Y, Yoshimura K, Yamamoto T, Suzuki H, Yokomuro K, et al. Detection of nephritis strain-associated streptokinase by monoclonal antibodies. J Med Microbiol 1991; 35:60–63.
19. Blake MS, Johnston KH, Russell-Jones GJ, Gotschlich EC. A rapid, sensitive method for detection of alkaline phosphatase-conjugated anti-antibody on Western blots. Anal Biochem 1984;136:175–9.
20. Reynolds ES. The use of lead citrate at high pH as an electron-opaque stain in electron microscopy. J Cell Biol 1963;17:208–12.
21. Farrand S, Hotze E, Friese P, Hollingshead SK, Smith DF, Cummings RD, et al. Characterization of a streptococcal cholesterol-dependent cytolysin with a Lewis y and b specific lectin domain. Biochemistry 2008;47:7097–107.
22. Nagamune H, Ohnishi C, Katsuura A, Fushitani K, Whiley RA, Tsuji A, et al. Intermedilysin, a

novel cytotoxin specific for human cells secreted by Streptococcus intermedius UNS46 isolated from a human liver abscess. Infect Immun 1996;64:3093–100.
23. Jefferies J, Nieminen L, Kirkham L-A, Johnston C, Smith A, Mitchell TJ. Identification of a secreted cholesterol-dependent cytolysin (mitilysin) from Streptococcus mitis. J Bacteriol 2007; 189:627–32.
24. Gelber SE, Aguilar JL, Lewis KL, Ratner AJ. Functional and phylogenetic characterization of vaginolysin, the human-specific cytolysin from Gardnerella vaginalis. J Bacteriol 2008;190:3896–903.
25. Dubail I, Autret N, Beretti J-L, Kayal S, Berche P, Charbit A. Functional assembly of two membrane-binding domains in listeriolysin O, the cytolysin of Listeria monocytogenes. Microbiology 2001;147:2679–88.
26. Heuck AP, Tweten RK, Johnson AE. Beta-barrel pore-forming toxins: intriguing dimorphic proteins. Biochemistry 2001;40:9065–73.
27. Rossjohn J, Feil SC, McKinstry WJ, Tweten RK, Parker MW. Structure of a cholesterol-binding, thiol-activated cytolysin and a model of its membrane form. Cell 1997;89:685–92.
28. Havarstein LS, Hakenbeck R, Gaustad P. Natural competence in the genus *Streptococcus*; evidence that streptococci can change phenotype by interspecies recombinational exchange. J Bacteriol 1997;179:6589–94.
29. Nakamura M, Sekino N, Iwamoto M, Ohno-Iwashita Y. Interaction of theta-toxin (perfringolysin O), a cholesterol-binding cytolysin, with liposomal membranes: change in the aromatic side chains upon binding and insertion. Biochemistry 1995;34:6513–20.
30. Nagamune H, Ohkura K, Sukeno A, Cowan G, Mitchell TJ, Ito W, et al. The human-specific action of inermedilysin, a homology of streptolysin O, is dictated by domain 4 of the protein. Microbiol Immunol 2004;48:677–92.

APPENDIX

The content of this manuscript was presented in part at the AMS Conference on Streptococcal genetics, Vichy, France, April 26–19, 1998, at the XIV Lancefield International Symposium on Streptococci and Streptococcal Diseases, Auckland, New Zealand, October 11–15, 1999, and at the XVII Lancefield International Symposium on Streptococci and Streptococcal Diseases, Porto Heli, Greece, June 22–26, 2008.

Immunobiology xxx (2012) xxx–xxx

Contents lists available at SciVerse ScienceDirect

Immunobiology

journal homepage: www.elsevier.de/imbio

Disruption of maternal immune balance maintained by innate DC subsets results in spontaneous pregnancy loss in mice

Yasuyuki Negishi[a,b], Ayako Wakabayashi[a], Masumi Shimizu[a], Tomoko Ichikawa[a,b], Yoshihiro Kumagai[a], Toshiyuki Takeshita[b], Hidemi Takahashi[a,*]

[a] Department of Microbiology and Immunology, Nippon Medical School, Tokyo 113-8602, Japan
[b] Department of Obstetrics and Gynecology, Nippon Medical School, Tokyo 113-8602, Japan

ARTICLE INFO

Article history:
Received 6 June 2011
Received in revised form
19 November 2011
Accepted 6 January 2012

Key words:
DC
Pregnancy
Progesterone
Th1/Th2 balance
DEC-205
33D1
Dendritic cell inhibitory receptor-2 (DCIR2)
Paraaortic lymph nodes (PALNs)

ABSTRACT

Dendritic cells (DCs) play an important role in providing an appropriate fetal/maternal balance between Th1 and Th2 during pregnancy. The Th1/Th2 balance seems to be regulated mainly by two distinct DC subsets, DEC-205$^+$ DCs having the capacity to establish Th1 polarization and 33D1$^+$ DCs to induce Th2 dominance. Pregnancy is established and maintained by maternal hormones, such as progesterone and estrogen, and the balance of DC subtypes was affected mainly by progesterone, which induced a dose-dependent reduction of the DEC-205/33D1 ratio together with/without a stable amount of estrogen. The DEC-205/33D1 ratio decreased gradually with the progress of pregnancy and rapid augmentation of the ratio was seen around delivery *in vivo*. Here, we demonstrate that depletion of 33D1$^+$ DCs during the perinatal period caused substantial fetal loss probably mediated through Th1 up-regulation via transient IL-12 secretion, and pre-administration of progesterone could rescue the fetal loss. Similar miscarriages were also observed when pregnant mice were intraperitoneally (i.p.) injected twice with IL-12 on Gd 9.5 and 10.5. Moreover, prior inoculation of progesterone suppressed the enhanced serum IL-12 production in mice treated with 33D1 antibody, indicating that progesterone might inhibit temporal IL-12 secretion around Gd 10.5 and miscarriage was avoided. These findings suggest the importance of balancing DC subsets during pregnancy and reveal that we can avoid miscarriage by manipulating the activity of the DC subpopulation of pregnant individuals with maternal hormones.

Introduction

The maternal immune response is crucial for a successful pregnancy. Immunity against fetal semi-alloantigens encoded by paternal genes is thought to be tolerated, although it should protect the fetus from infections during pregnancy. Nevertheless, at a suitable time, the fetus is safely delivered from the mother. In this regard, the appropriate balance between Th1 and Th2 has been discussed during pregnancy. Indeed, it is considered that predominant Th2 immunity is essential for maintaining a successful pregnancy (Blois et al. 2004; Piccinni et al. 1998). Thus, under Th2 dominancy, the symptoms of many diseases correlated with autoimmune disorders are altered during pregnancy. For example, systemic lupus erythematosus (SLE), associated with Th2 cytokine production, tends to flare and worsen (Doria et al. 2008), while rheumatoid arthritis (RA), linked to Th1 cytokines, is apt to improve during pregnancy (Doria et al. 2006).

Innate DCs are the most powerful antigen-presenting cells (APCs) and are critical for the induction of primary immune responses. Pattern recognition receptors (PRRs), such as TLRs and lectin receptors on DCs, are important to recognize pathogen-associated molecular patterns (PAMPs) (Steinman 1991). The role of such DCs has also been argued in the feto-maternal immune system (Karsten et al. 2009; Laskarin et al. 2007) and many groups have speculated the actual roles of DCs within the uterus during pregnancy (Bizargity and Bonney 2009; Blois et al. 2007; Collins et al. 2009). Moreover, it has recently been reported that tissue-residing DCs, entrapped in the decidua, might minimize immunogenic T cell activation against fetal/placental antigens in the draining lymph nodes and establish tolerance against the embryo (Collins et al. 2009). Furthermore, it has recently been reported that depletion of uterine DCs altered decidual angiogenesis and caused embryo resorption even in a T cell-deficient pregnant state (Plaks et al. 2008; Pollard 2008). These findings strongly suggest the direct involvement of decidual DCs in the maintenance of pregnancy and reveal the possibility that pregnancy is mediated without specific

* Corresponding author at: Department of Microbiology and Immunology, Nippon Medical School, 1-1-5 Sendagi, Bunkyo-ku, Tokyo 113-8602, Japan.
Tel.: +81 3 3822 2131x5381; fax: +81 3 3316 1904.
E-mail address: htkuhkai@nms.ac.jp (H. Takahashi).

0171-2985/$ – see front matter © 2012 Elsevier GmbH. All rights reserved.
doi:10.1016/j.imbio.2012.01.011

acquired T cell immunity that may cause substantial damage to internal foreign organs, such as transplanted semi-allogeneic grafts (Nagler et al. 2003). Nevertheless, safely delivered newborn babies generally have not suffered any damage during pregnancy even in the semi-allogeneic state, indicating that allogeneic antigen-specific acquired immunity may not be a major factor for delivery. Moreover, the fact that syngeneic mating of mice can produce offspring in the absence of semi-allogeneic antigens in the fetus strongly suggests that allo-specific acquired immunity may be less related to normal delivery than expected; therefore, we examined the actual relationship of innate maternal DCs for the maintenance of pregnancy and the initiation of delivery.

Recently, two major distinct subsets of $CD11c^+$ DCs expressing their own Clec4a4 C-type lectin domain family 4, member a4, 33D1 (Dudziak et al. 2007) and LY75, DEC-205 (CD205) (Bozzacco et al. 2007), have been shown to regulate our immune responses *in vivo* (Figdor et al. 2002). $DEC\text{-}205^+$ DCs have the capacity to establish Th1 polarization, whereas $33D1^+$ DCs, recognizing dendritic cell inhibitory receptor-2 (DCIR2) (Dudziak et al. 2007), create Th2 polarization (Moriya et al. 2010). Based on such findings, we examined the kinetics of the expression of C-type lectin receptors on DCs during the perinatal period and analyzed the influences of these receptor-positive DCs on the maintenance of pregnancy requiring an appropriate Th1/Th2 balance.

In the present study, we studied the kinetics of murine DC subsets, $DEC\text{-}205^+$ and $33D1^+$ DCs, in the spleen during the perinatal period and found sharp augmentation of the DEC-205/33D1 ratio just after delivery, which was mainly caused by the rapid decease of $33D1^+$ DCs and the prompt increase of $DEC\text{-}205^+$ DCs. Surprisingly, apparent fetal loss could be induced reproducibly by the depletion of $33D1^+$ DCs during the perinatal period. We also found that the balance of DC subtypes is profoundly affected by progesterone, which caused an apparent reduction of the DEC-205/33D1 ratio with increasing doses. Thus, we injected progesterone to see whether we could rescue the fetal loss generated through the depletion of $33D1^+$ DCs, and this was confirmed.

These findings demonstrate the importance of balancing the innate DC subsets during pregnancy and suggest that we may rescue miscarriages by manipulating the number and activity of the DC subpopulation in pregnant individuals with maternal hormones.

Materials and methods

Mice

Female BALB/c, male BALB/c, female C57BL/6, and male C57BL/6 mice were purchased from Charles River Laboratories (Kanagawa, Japan), maintained in micro-isolator cages under specific pathogen-free conditions, and fed autoclaved laboratory chow and water with a 12 h light–dark cycle. Virgin females (8–12 weeks) were mated with males. The day when a vaginal plug was detected in the mated females was determined as gestational day (Gd) 0.5. Pregnant mice were sacrificed on Gd 5.5, 10.5, 15.5, 18.5, just after delivery, and 5 days after delivery. Spleen, paraaortic lymph nodes (PALNs), and the uterus were removed from pregnant mice, and cells were harvested from these organs. All animal experiments were performed according to guidelines for the care and use of laboratory animals set by the National Institutes of Health (NIH, MD) and approved by the Review Board of Nippon Medical School (Tokyo, Japan).

Cell preparation and flow cytometry analysis

The decidua of the uterus was removed together with the placenta using ophthalmic scissors under a stereoscopic microscope. After removing the spleen, PALNs, and decidua, the tissues were cut into small pieces and incubated with 1 mg/ml collagenase D (Roche, Basel, Switzerland) at 37 °C for 45 min. The obtained cells were finely mashed, passed through nylon mesh, and washed with RPMI 1640 medium (Sigma–Aldrich, St Louis, MO). To eliminate contaminated red blood cells, the cells were suspended with 0.1× PBS (pH 7.2, 0.15 M NaCl) for osmotic hemolysis and an equal amount of 2× PBS was added immediately after lysis. Cells were centrifuged (1200 rpm, 20 °C, 8 min) and collected. After incubation with Fc blocker (clone 24G2; American Type Culture Collection (ATCC), Manassas, VA) for 15 min to avoid non-specific antibody binding with Fc receptors, the cells were stained for 30 min at 4 °C with 50 μl diluted FITC- or PE-labeled monoclonal antibodies (mAbs): FITC-conjugated anti-DEC-205 (clone: NLDC-145 (rat IgG2a); Cedarlane, Ontario, Canada), PE-conjugated 33D1 (clone: 33D1 (rat IgG2b); BD Biosciences, San Diego, CA), FITC-conjugated anti-CD11c (clone: N418; BD Biosciences), PE-conjugated anti-CD11c (clone: N418; BD Biosciences), FITC-conjugated anti-CD11b (clone: M1/70; eBioscience, San Diego, CA), PE- and FITC-conjugated anti-CD8α (clone: 53-6.7; BioLegend, San Diego, CA), FITC-conjugated anti-CD4 (clone GK1.5; eBioscience), PE-conjugated anti CD4 (clone: RM4.5; BD Biosciences), APC-conjugated anti-CD3 (clone 145-2C11; BioLegend), Biotin-conjugated anti CD69 (clone: H1.2F3; BD Biosciences), APC Cy7-conjugated Streptavidin (BD Biosciences), and FITC-conjugated anti-CD25 (clone 7D4; BD Biosciences). After washing twice with FACS buffer solution, dead cells were determined using propidium iodide (PI; Sigma–Aldrich) or 7-amino-actinomycin D viability dye (Beckman Coulter), and stained cells were analyzed with FACScan using the CellQuest program (BD Biosciences) or analyzed by FACScanto II (BD Biosciences) with FlowJo software (Tree Star, Ashland, OR). DCs were gated according to their FSC/SSC characteristics. PE- and FITC-labeled rat IgG2a isotype-matched control antibodies (clone: RTK2758; BioLegend) and rat IgG2b isotype-matched control antibodies (clone: RTK4530; BioLegend) were used as negative controls to set the gate thresholds of each measurement.

Effect of progesterone and estradiol on bone marrow-derived DCs

Bone marrow cells were obtained from the femur of virgin female BALB/c mice. Cells suspended in RPMI 1640 were centrifuged (1500 rpm, 20 °C, 5 min) and collected. The cells were then re-suspended in 0.1× PBS for osmotic hemolysis and an equal amount of 2× PBS was added immediately to eliminate contaminating red blood cells. Cells were centrifuged (1500 rpm, 20 °C, 5 min) and collected. Obtained bone marrow cells were cultured at a density of 1×10^6 cells in 1 ml RPMI-1640-based culture medium (Takahashi et al. 1996) supplemented with 2 mM L-glutamine (Sigma–Aldrich), 1 mM sodium pyruvate (Invitrogen Life Technologies, Carlsbad, CA), 0.1 mM nonessential amino acid (Invitrogen Life Technologies), a mixture of vitamins (Invitrogen Life Technologies), 1 mM HEPES (Invitrogen Life Technologies), 100 U/ml penicillin (Invitrogen Life Technologies), 100 μg/ml streptomycin (Invitrogen Life Technologies), 50 mM 2-ME (Sigma–Aldrich) and heat-inactivated 10% fetal calf serum (FCS; Hyclone, Logan, UT) (ref), containing 10 ng/ml GM-CSF (Biosource International, Camarillo, CA) and 10 ng/ml IL-4 (Biosource International, Inc.) in 24-well flat-bottom multiwall plates (BD Biosciences) at 37 °C. Progesterone or estradiol (both from Sigma–Aldrich) was added at the following concentrations: 0.1 μg/ml, 1 μg/ml, and 3 μg/ml at the time of starting culture. On day 2, the culture medium was replaced with fresh medium and the floating cells (e.g. lymphocytes) were removed. On day 5, floating and loosely adherent cells were collected, washed, and analyzed by FACScan.

Please cite this article in press as: Negishi, Y., et al., Disruption of maternal immune balance maintained by innate DC subsets results in spontaneous pregnancy loss in mice. Immunobiology (2012), doi:10.1016/j.imbio.2012.01.011